Photoinduced Electron- and Energy-Transfer Processes Occurring within Porphyrin–Metal–Bisterpyridyl Conjugates

Jean-Paul Collin,† Anthony Harriman,*‡ Valérie Heitz,† Fabrice Odobel,† and Jean-Pierre Sauvage*,†

Contribution from the Faculté de Chimie, Université Louis Pasteur, 1 rue Blaise Pascal, 67000 Strasbourg, France, and Center for Fast Kinetics Research, The University of Texas at Austin, Austin, Texas 78712

Received December 23, 1993®

Abstract: Photophysical properties have been measured for zinc and free-base porphyrins covalently linked to ruthenium(II) or rhodium(III) bisterpyridyl complexes using ultrafast transient absorption spectroscopy. The appended metal complex quenches porphyrin fluorescence due to rapid intramolecular electron transfer. For directly coupled systems, the rate of photoinduced electron transfer ($k \approx 10^{12}$ s^{-1}) approaches the inverse of the solvent reorientation time in solvents that relax rapidly but greatly exceeds the relaxation rate in ethanol at low temperature. These electron-transfer processes, which remain rapid in an ethanol glass at 77 K, are considered in terms of the model introduced by Sumi and Marcus (*J. Chem. Phys.* **1986**, *84*, 4894). Inserting a phenyl ring between the reactants decreases the extent of their mutual electronic coupling so that the rates of electron transfer decrease. Because of the large amount of energy that must be dissipated, charge recombination is relatively slow in these latter systems, and the observed kinetic data can be well described in terms of current nonadiabatic electron transfer theory. In particular, the phenyl-bridged, ruthenium(II) bisterpyridyl-based conjugate possesses properties that appear suitable for its use as a molecular bridge in multicomponent photosynthetic systems where it should facilitate rapid long-range, multistep electron transfer. This latter conjugate also demonstrates Dexter-type triplet energy transfer from metal complex to porphyrin.

The assemblage of multicomponent photoactive arrays by logical but noncovalent interlocking of individual molecular modules is an attractive means by which to construct organized artificial photosynthetic reaction centers. It is necessary, however, to identify appropriate noncovalent bridges that facilitate close positioning of specific molecular subunits in a well-defined sequence. Indeed, while considerable success has been achieved with covalent linkages,[1-4] there are relatively few examples in which noncovalent bonding has been utilized to assemble effective photodiodes or higher oligomers. Recent studies have concentrated on bridging units incorporating hydrogen bonds,[5] electrostatic attractive forces,[6] van der Waals[7] or charge-transfer interactions,[8] or cation chelation.[9] The latter approach, in particular, demonstrates genuine potential for practical exploitation since it provides a simple method for spatial alignment of reactive subunits, as illustrated below:

(1)

Several such systems have now been synthesized[9-11] and shown to facilitate photoinduced electron- and/or energy-transfer reactions. Here, we extend the scope of these prototypes by reporting the photochemistry of systems in which a metal bisterpyridyl complex is closely associated with a porphyrin chromophore. The primary objective of this work is to identify metal complexes that can be used as building blocks for construction of linear arrays of (metallo)porphyrins, and, as a first step, we concentrate on exploring the photophysics of the porphyrin–metal complex diode. In this respect it should be noted that difunctionalized terpyridyl units, unlike the corresponding 2,2′-bipyridyl units, are especially valuable modules for engineering of rigid molecular wires containing metal centers. Several porphyrin–ruthenium(II) tris(2,2′-bipyridyl) conjugates have been described previously,[12,13] and it has been shown that the appended porphyrin extinguishes luminescence from the ruthenium(II) chelate. The mechanism for this quenching effect was not discussed, but we have shown that, for our system, efficient intramolecular triplet energy transfer occurs from the ruthenium(II) chelate to the adjacent porphyrin. We have further shown that intramolecular electron transfer takes place upon illumination of the porphyrin subunit; this process was not observed with the prior systems.[12,13]

Positioning photo- or redox-active subunits in close proximity to each other can result in strong electronic interaction between the components. This, in turn, may complicate detailed analysis of the electron-transfer rates. Thus, while theoretical understanding of electron-transfer rates involving weakly coupled reactants has advanced enormously in recent years,[14] much remains to be learned about the dynamics of electron transfer occurring in the adiabatic regime.[15] Under specific conditions,

† Université Louis Pasteur.

‡ The University of Texas at Austin.

® Abstract published in *Advance ACS Abstracts,* May 15, 1994.

(1) Miller, J. R. *Nouv. J. Chim.* **1987**, *11*, 83.

(2) Balzani, V.; Scandola, F. *Supramolecular Chemistry*; Horwood: Chichester, 1991.

(3) Gust, D.; Moore, T. A. *Science* **1989**, *244*, 35.

(4) Harriman, A. *Photosensitization and Photocatalysis Using Inorganic and Organometallic Compounds*; Kalyanasundaram, K., Gratzel, M., Eds.; Kluwer: Dordrecht, 1993; p 273.

(5) (a) Tecilla, P.; Dixon, R. P.; Slobodkin, G.; Alavi, D. S.; Waldeck, D. H.; Hamilton, A. D. *J. Am. Chem. Soc.* **1990**, *112*, 9408. (b) Harriman, A.; Magda, D.; Sessler, J. L. *J. Phys. Chem.* **1991**, *95*, 1530. (c) Harriman, A.; Kubo, Y.; Sessler, J. L. *J. Am. Chem. Soc.* **1992**, *114*, 388. (d) Aoyama, Y.; Asakawa, M.; Matsui, Y.; Ogoshi, H. *J. Am. Chem. Soc.* **1991**, *13*, 6233. (e) Turro, C.; Chang, C. K.; Leroi, G.; Cukier, R. I.; Nocera, D. G. *J. Am. Chem. Soc.* **1992**, *114*, 4013.

(6) (a) Brun, A. M.; Harriman, A.; Hubig, S. M. *J. Phys. Chem.* **1992**, *96*, 254. (b) Segawa, H.; Takehara, C.; Honda, K.; Shimidzu, T.; Asahi, T.; Mataga, N. *J. Phys. Chem.* **1992**, *96*, 503.

(7) (a) Benniston, A. C.; Harriman, A.; Philp, D.; Stoddart, J. F. *J. Am. Chem. Soc.* **1993**, *115*, 5298. (b) Benniston, A. C.; Harriman, A. *Angew. Chem., Int. Ed. Engl.* **1993**, *32*, 1459.

(8) Mataga, N.; Kanda, Y.; Okada, T. *J. Phys. Chem.* **1986**, *90*, 3880.

(9) (a) Brun, A. M.; Atherton, S. J.; Harriman, A.; Heitz, V.; Sauvage, J.-P. *J. Am. Chem. Soc.* **1992**, *114*, 4632. (b) Odobel, F.; Sauvage, J.-P.; Harriman, A. *Tetrahedron Lett.* **1993**, *34*, 8113.

(10) Barigelletti, F.; Flamigni, L.; Balzani, V.; Collin, J.-P.; Sauvage, J.-P.; Sour, A.; Constable, E. C.; Cargill Thompson, A. M. W. *J. Chem. Soc., Chem. Commun.* **1993**, 942.

(11) (a) De Cola, L.; Barigelletti, F.; Balzani, V.; Belser, P.; von Zelewsky, Steel, C.; Frank, M.; Vögtle, F. *Supramolecular Chemistry*; Balzani, V., De Cola, L., Eds.; NATO ASI Series C, Kluwer: Dordrecht, 1992; Vol. 371, p 157. (b) De Cola, L.; Balzani, V.; Barigelletti, F.; Flamigni, L.; Belser, P.; von Zelewsky, A.; Frank, M.; Vögtle, F. *Inorg. Chem.* **1993**, *32*, 5228.

(12) Hamilton, A. D.; Rubin, H.-D.; Bocarsly, A. B. *J. Am. Chem. Soc.* **1984**, *106*, 7255.

(13) Sessler, J. L.; Capuano, V. L.; Burrell, A. K. *Inorg. Chim. Acta* **1993**, *204*, 93.

0002-7863/94/1516-5679$04.50/0

rates of electron transfer may correspond to the dielectric relaxation rate of the solvent[16] but can exceed reorientation times in solvents which relax slowly.[17] In the latter case, high-frequency intramolecular modes coupled to electron transfer are believed to promote reaction. There are additional examples in which the rate of electron transfer scales with, but is much slower than, the inverse reorientation time of the solvent.[18] Furthermore, it is now recognized that electron transfer can take place along an intramolecular vibrational coordinate which is essentially independent of solvent in certain cases.[19] Indeed, Barbara and co-workers[20] have described a system for which the rate of electron transfer exhibits a weak temperature dependence that persists beyond the glass transition temperature of the solvent and for which the rate of electron transfer far exceeds dielectric relaxation of the solvent. We have observed comparable behavior for directly coupled porphyrin–rhodium(III) bisterpyridyl conjugates in which efficient quenching of the porphyrin excited singlet state occurs even in an ethanol glass at 77 K. Positioning a phenyl ring between porphyrin and terpyridyl ligand decreases the rates of electron transfer, especially for charge recombination. These latter systems appear to be promising modules for construction of linear multicomponent arrays.

Experimental Section

Materials. Solvents used for spectroscopic studies were of the highest available commercial grade and were fractionally distilled from appropriate drying agents before use. Pyrrole and *N,N*-dimethylformamide (DMF) were purified by distillation under reduced pressure over KOH, and all the other solvents and chemicals were used as purchased. Porphyrinic derivatives were protected from light by aluminum foil during purification on chromatography columns and during heating.

Compounds. 4′-Tolyl-2,2′:6′,2″-terpyridine[21] (**2**), 4′-[((trifluoromethyl)sulfonyl)oxy]-2,2′:6′,2″-terpyridine,[22] 4′-[(4-bromomethyl)-phenyl]-2,2′:6′,2″-terpyridine,[21] 3,5-di-*tert*-butylbenzaldehyde,[23] 3′-diethyl-4,4′-dimethyl-2,2′-dipyrrylmethane,[24] rhodium(III) bis-4′-tolyl-2,2′:6′,2″-terpyridine trichloride,[25] 5,15-((3,5-di-*tert*-butyl)phenyl)-3,7,13,17-tetraethyl-2,8,12,18-tetramethylporphyrin,[26] (**9**) and ruthenium(III) bis-4′-tolyl-2,2′:6′,2″-terpyridine trichloride[21] were prepared according to literature procedures. Tetra-5,10,15,20-((3,5-di-*tert*-butyl)phenyl)porphyrin (**7**) and 5,15-((3,5-di-*tert*-butyl)phenyl)-3,7,13,17-tetraethyl-2,8,-12,18-tetramethylporphyrin (**9**) were metalated with zinc(II) according to a general method.[27]

Anion Exchange Procedure. The complex was dissolved in the minimum amount of acetonitrile, and the same volume of a saturated aqueous solution of KPF_6 (about 0.6 g in 100 mL) was added. This solution was allowed to stand for 15 min without stirring. Water (three times the volume of acetonitrile) was added, and after standing for 15 min the precipitate was filtered, washed with water, and redissolved in acetonitrile. After drying with Na_2SO_4 and removal of the solvent, the complex was recovered as the PF_6^- salt. This operation was repeated if anion exchange was incomplete (as checked by TLC).

4′-Methyl-2,2′:6′,2″-terpyridine (1). A mixture of 4′-[((trifluoromethyl)sulfonyl)oxy]-2,2′:6′,2″-terpyridine[22a] (17.7 g, 46.5 mmol), tetramethyltin (8.31 g, 46.5 mmol) and lithium chloride (1 g, 0.14 mmol) in dimethylformamide (150 mL) was stirred at 130 °C for 3 h under argon. The reaction mixture was then stirred for 30 min with a mixture of cold water (600 mL) and an aqueous solution of ammonia (10%, 100 mL). The precipitate was filtered and washed several times with cold water until neutrality was reached, dissolved in CH_2Cl_2, and dried over $MgSO_4$. Evaporation of the solvent resulted in a pale yellow solid which was chromatographed on alumina using a hexane/ethyl acetate mixture (9/1) as eluent to afford 10 g of **1** (87%). ^1H NMR data were in agreement with those reported previously.[22b]

4′-Formyl-2,2′:6′,2″-terpyridine. Methylterpyridine **1** (0.10 g, 0.4 mmol), iodine (0.10 g, 0.4 mmol), trifluoroacetic acid (0.12 mL, 1.2 mmol), and *tert*-butyl iodide (20 mL, 0.16 mmol) were dissolved in dry dimethyl sulfoxide (DMSO) (2 mL) under argon, and the mixture was heated at 110 °C for 12 h. Subsequently, DMSO was removed under vacuum, and the residue was dissolved in CH_2Cl_2 and washed first with $Na_2S_2O_3$ solution (0.1 N), then with 10% aqueous sodium carbonate, and finally with water. The organic layer was dried over $MgSO_4$. Evaporation of the solvent yielded 60 mg of formylterpyridine (57%): ^1H NMR (200 MHz, CD_2Cl_2) δ = 10.26 (s, 1H), 8.86 (s, 2H), 8.70 (d, d, d, 2H, J = 4.8, 1.8 and 0.8 Hz), 8.64 (d, d, d, 2H, J = 7.9, 1.0, and 1.0 Hz), 7.90 (d, d, d, 2H, J = 7.7, 1.9, and 1.9 Hz), 7.40 (d, d, d, 2H, J = 7.5, 4.8, and 1.3 Hz); mp 170 °C; IR ($CHCl_3$) ν = 1715 cm^{-1}.

5-[4′-(2,2′:6′,2″-Terpyridinyl)]tris[10,15,20-[(3,5-di-*tert*-butyl)phenyl]]-porphyrin (3). A mixture of formylterpyridine (0.2 g, 0.70 mmol), 3,5-di-*tert*-butylbenzaldehyde[23] (3 g, 13.7 mmol), and pyrrole (1 mL, 14.4 mmol) in propionic acid (30 mL) was refluxed for 2 h. Propionic acid was removed by azeotropic distillation with toluene in *vacuo*. The resultant red-brown solid was dissolved in CH_2Cl_2 (200 mL) and washed twice with 10% aqueous sodium carbonate and finally three times with water. The organic layer was dried over $MgSO_4$. Chromatography of the crude material first on alumina (hexane/ethyl acetate, 99.6/0.4 as eluent) and then on silica gel (CH_2Cl_2/MeOH, 95/5 as eluent) gave 55 mg of porphyrin **3** (7%): ^1H NMR (400 MHz, CD_2Cl_2) δ = 9.39 (s, 2H), 9.00 (d, d, d, 2H, J = 7.9, 0.9 and 0.9 Hz), 8.99 (s, 2H), 8.97 (s, 2H), 8.95 (s, 4H), 8.67 (d, d, d, 2H, J = 4.6, 1.7, and 0.9 Hz), 8.15 (d, 6H, J = 1.8 Hz), 8.02 (d, d, d, 2H, J = 7.7, 7.7, and 1.8 Hz), 7.89 (t, 3H, J = 1.8 Hz), 7.40 (d, d, d, 2H, J = 7.5, 4.7, and 1.2 Hz), 1.57 (s, 18 H), 1.56 (s, 36H), –2.67 (s, 2H); FAB-MS (*m*-nitrobenzyl alcohol (NBA) matrix) m/z = 1106.5 ($C_{77}H_{83}N_7^+$ requires 1106.6); UV–vis (CH_2Cl_2) λ_{max} (nm) 422, 518, 553, 592, 648.

4′-Phenylcarbonyl-2,2′:6′,2″-terpyridine. A mixture of 4′-(bromomethyl)phenyl-2,2′:6′,2″-terpyridine[21] (1 g, 2.5 mmol) and 4 equiv of hexamethylenetetramine (1.4 g, 10 mmol) was refluxed in a C_2H_5OH/H_2O mixture (2/1) for 25 h. HCl (1 mL) was added carefully, and reflux was continued for 0.5 h. After cooling and neutralization with Na_2CO_3 the white solid obtained was chromatographed on a silica gel column (CH_2Cl_2/MeOH, 99/1 as eluent) to afford 0.36 g of pure product (43%): ^1H NMR (200 MHz, CD_2Cl_2) δ = 10.10 (s, 1H), 8.80 (s, 2H), 8.71 (m, 4H), 8.05 (s, 4H), 7.95 (td, 2H, J = 8 and 1.2 Hz), 7.38 (d, d, d, 2H, J = 11.5 and 2 Hz); FAB-MS m/z = 337 ($C_{22}H_{15}N_3O^+$ requires 337.4).

5,15-Bis[4-(4′-phenyl-2,2′:6′,2″-terpyridinyl)]-3,7,13,17-tetraethyl-2,8,12,18-tetramethylporphyrin (4). A mixture of 3,3′-diethyl-4,4′-dimethyl-2,2′-dipyrrylmethane[24] (0.337 g, 1.64 mmol), 4′-phenylcarbonyl-2,2′:6′,2″-terpyridine (0.554 g, 1.64 mmol), and trifluoroacetic acid (60 μL) in CH_2Cl_2 (35 mL) was stirred under argon at room temperature for 24 h, leading to formation of a red solid. Chloranil (1 g) was added, and the resultant black solution was refluxed for 1 h. An aqueous solution of Na_2CO_3 (2 g in 200 mL) was added, and the mixture was stirred for 0.5 h. The crude product obtained after extraction (CH_2Cl_2; 2 × 200 mL) was washed with ethanol. Two recrystallizations from a CH_2Cl_2/C_2H_5OH mixture (2/1) afforded the pure bisterpyridylporphyrin as a red solid (0.384 g, 42%): ^1H NMR (200 MHz, $CDCl_3$) δ = 10.28 (s, 2H), 9.09 (s, 4H), 8.82 (m, 8H), 8.32 (d, 4H, 8.4 Hz), 8.25 (d, 4H, 8.4 Hz), 7.97 (td, 4H, J = 7.7 and 1.8 Hz), 7.43 (d, d, d, 4H, J = 8, 4.6 and 1 Hz), 4.05 (q, 8H), 2.58 (s, 12H), 1.80 (t, 12H, 7.6 Hz), –2.35 (s, 2H); FAB-MS (NBA) m/z = 1093.2 ($C_{74}H_{65}N_{10}^+$ requires 1093); UV–vis ($CHCl_3$) λ_{max} (nm) 410, 509, 542, 575, 627.

(14) (a) Marcus, R. A.; Sutin, N. *Biochim. Biophys. Acta* **1985**, *811*, 265. (b) Kakitani, K.; Mataga, N. *J. Phys. Chem.* **1985**, *89*, 4752. (c) Beratin, D. N.; Onuchic, J. N.; Hopfield, J. J. *J. Chem. Phys.* **1985**, *83*, 5325.
(15) Doorn, S. K.; Dyer, R. B.; Stoutland, P. O.; Woodruff, W. H. *J. Am. Chem. Soc.* **1993**, *115*, 6398.
(16) (a) Simon, J. D.; Su, S.-G. *J. Chem. Phys.* **1987**, *87*, 7016. (b) Simon, J. D.; Su, S.-G. *J. Phys. Chem.* **1988**, *92*, 2395. (c) Masad, A.; Huppert, D.; Kosower, E. M. *Chem. Phys.* **1990**, *144*, 391.
(17) (a) Simon, J. D.; Su, S.-G. *Chem. Phys.* **1991**, *152*, 143. (b) Tominaga, K.; Walker, G. C.; Kang, T. J.; Barbara, P. F. *J. Phys. Chem.* **1991**, *95*, 10485.
(18) (a) Calef, D. F.; Wolynes, P. G. *J. Phys. Chem.* **1983**, *87*, 3387. (b) Calef, D. F.; Wolynes, P. G. *J. Chem. Phys.* **1983**, *78*, 470. (c) Zaleski, J. M.; Chang, C. K.; Leroi, G. E.; Cukier, R. I.; Nocera, D. G. *J. Am. Chem. Soc.* **1992**, *114*, 3564.
(19) Sumi, H.; Marcus, R. A. *J. Chem. Phys.* **1986**, *84*, 4894.
(20) (a) Akesson, E.; Walker, G. C.; Barbara, P. F. *J. Chem. Phys.* **1991**, *95*, 4188. (b) Tominaga, K.; Walker, G. C.; Jarzeba, W.; Barbara, P. F. *J. Phys. Chem.* **1991**, *95*, 10475. (c) Walker, G. C.; Akesson, E.; Johnson, A. E.; Levinger, N. E.; Barbara, P. F. *J. Phys. Chem.* **1992**, *96*, 3728.
(21) Collin, J.-P.; Guillerez, S.; Sauvage, J.-P.; Barigelletti, F.; De Cola, L.; Flamigni, L.; Balzani, V. *Inorg. Chem.* **1991**, *30*, 4230.
(22) (a) Potts, K. T.; Honwar, D. J. *J. Org. Chem.* **1991**, *56*, 4815. (b) Bates, R. B.; Gordon III, B.; Keller, P. C.; Rund, J. V.; Mills, N. S. *J. Org. Chem.* **1980**, *45*, 168.
(23) Newman, M. S.; Lee, L. F. *J. Org. Chem.* **1972**, *26*, 4468.
(24) Young, R.; Chang, C. K. *J. Am. Chem. Soc.* **1986**, *107*, 898.
(25) Collin, J.-P.; Jouaiti, A.; Sauvage, J.-P. *J. Electroanal. Chem.* **1990**, *286*, 76.
(26) Osuka, A.; Liu, B.-L.; Maruyama, K. *J. Org. Chem.* **1993**, *58*, 3582.
(27) Smith, K. M. *Porphyrins and Metalloporphyrins*; Elsevier: Amsterdam, 1975.

Rhodium(III) 4'-Methyl-2,2':6',2''-terpyridine Trichloride. To 100 mL of absolute ethanol in a round-bottomed flask was added rhodium trichloride trihydrate (110 mg, 0.42 mmol) and methylterpyridine **1** (110 mg, 0.44 mmol). This mixture was heated under reflux for 2.5 h. The reaction mixture was cooled to room temperature and the fine yellow precipitate was filtered and washed several times with ethanol and ether. It was then dried in *vacuo*. Pure rhodium methylterpyridine trichloride (176 mg) was prepared by this method (92%): ^{1}H NMR (200 MHz, DMSO-d_6) δ = 9.28 (d, 2H, J = 5.6 Hz), 8.78 (s, 2H), 8.68 (d, d, d, 2H, J = 7.9, 7.9, and 1.5 Hz), 8.36 (d, d, d, 2H, J = 7.9, 7.9, and 1.5 Hz), 7.92 (d, d, d, 2H, J = 7.7, 5.6, and 1.3 Hz), 2.77 (s, 3H); FAB-MS (NBA matrix) m/z = 419.8 ($C_{16}H_{13}N_3RhCl_2^+$ requires 419.9).

Rhodium(III) 5-[4'-(2,2':6',2''-Terpyridinyl)]tris[10,15,20-[(3,5-di-*tert*-butyl)phenyl]]porphyrin 4'-Methyl-2,2':6',2''-terpyridine 3+ (11). A suspension of rhodium methylterpyridine trichloride (17.6 mg, 0.039 mmol) and silver tetrafluoroborate (29.3 mg, 0.15 mmol) in 35 mL of an acetone/absolute methanol (6/1) mixture were refluxed under argon for 3.5 h. After cooling and filtration, the resultant precipitate of AgCl was washed with absolute ethanol (20 mL), and the acetone was removed from the filtrate under vacuum. Then, the second ligand **5** (40 mg, 0.039 mmol) was added to the solution, and the mixture was refluxed under argon for 17 h. The solvent was evaporated, the residue was dissolved in acetonitrile, and anion exchange was performed. The crude brown-green product was purified by chromatography on silica gel eluting with a mixture of acetonitrile/water/saturated KNO_3 (90/10/0.5). After anionic exchange, 50 mg of compound **11** were obtained (70% yield): ^{1}H NMR (400 MHz, CD_3CN) δ = 9.75 (s, 2H), 9.43 (d, 2H, J = 4.8 Hz), 9.08 (d, 2H, J = 4.8 Hz), 8.93 (q, 4H, J = 4.8 Hz), 8.88 (d, 2H, J = 0.5 Hz), 8.67 (m, 4H), 8.37 (d, d, d, 2H, J = 7.9, 7.9, and 1.3 Hz), 8.22 (d, d, d, 2H, J = 7.9, 7.9, and 1.3 Hz), 8.16 (m, 2H), 8.16 (d, 4H, J = 1.8 Hz), 8.14 (t, 2H, J = 1.8 Hz), 7.98 (t, 2H, J = 1.9 Hz), 7.97 (t, 1H, J = 1.9 Hz), 7.80 (m, 2H), 7.73 (d, d, d, 2H, J = 7.4, 5.9, and 1.3 Hz), 7.57 (d, d, d, 2H, J = 7.4, 5.9, and 1.3 Hz), 3.09 (s, 3H), 1.55 (s, 36H), 1.55 (s, 18H), -2.61 (s, 2H); mp > 300 °C. ES-MS m/z = 485.9 ($C_{93}H_{96}N_{10}Rh^{3+}$ requires 485.6); UV-vis, (CH_3CN) λ_{max} (nm) 414, 519, 564, 590, 652.

Rhodium(III) 5-[4'-(2,2':6',2''-Terpyridinyl)]tris[10,15,20-[(3,5-di-*tert*-butyl)phenyl]] Zinc Porphyrin 4'-Methyl-2,2':6',2''-terpyridine 3+ Species 12. Compound **11** (21 mg, 0.011 mmol) and zinc acetate dihydrate (10 mg, 0.045 mmol) were dissolved in an absolute methanol/acetonitrile (5/2) mixture. The solution was stirred and refluxed under argon for 30 min. The course of reaction was followed by UV-visible absorption spectroscopy, and reflux was continued until the four Q-bands of the free-base porphyrin had been replaced by the characteristic two-banded spectrum of the zinc porphyrin. The solution was then cooled to room temperature, subjected to anion exchange, and chromatographed on silica gel with an acetonitrile/water/aqueous saturated KNO_3 (90/10/0.2) mixture as eluent to yield 20 mg (92%) of the metalated porphyrin: ^{1}H NMR (400 MHz, CD_3CN) δ = 9.74 (s, 2H), 9.42 (d, 2H, J = 4.7 Hz), 9.08 (d, 2H, J = 4.7 Hz), 8.92 (t, 4H, J = 4.8 Hz), 8.88 (s, 2H), 8.71 (s, 2H), 8.66 (s, 2H), 8.40 (d, d, d, 2H, J = 7.9, 7.9, and 1.5 Hz), 8.25 (d, d, d, 2H, J = 7.9, 7.9, and 1.5 Hz), 8.15 (d, 4H, J = 1.8 Hz), 8.14 (m, 2H), 8.12 (d, 2H, J = 1.8 Hz), 7.96 (t, 1H, J = 1.9 Hz), 7.94 (t, 2H, J = 1.9 Hz), 7.79 (m, 2H), 7.74 (m, 2H), 7.57 (m, 2H), 3.07 (s, 3H), 1.56 (s, 36H), 1.55 (s, 18H); mp > 300 °C; ES-MS m/z = 506.7 ($C_{93}H_{94}N_{10}RhZn^{3+}$ requires 506.7); UV-vis, (CH_3CN) λ_{max} (nm) 427, 564, 628.

Rhodium(III) Bis(4'-methyl-2,2':6',2''-terpyridine) 3+ (5). This complex was prepared in 50% yield following the procedure described for compound **11** and using methylterpyridine **1** instead of porphyrin **5**. The crude reaction product was purified by chromatography on silica gel by elution with an acetonitrile/water/saturated aqueous KNO_3 (80/20/3.5) mixture: ^{1}H NMR (200 MHz, CD_3CN) δ = 8.83 (d, 4H, J = 0.6 Hz), 8.61 (m, 4H), 8.25 (d, d, d, 4H, J = 7.9, 7.9, and 1.5 Hz), 7.69 (m, 4H), 7.47 (d, d, d, 4H, J = 7.6, 5.7, and 1.4 Hz), 2.99 (s, 6H); mp > 300 °C; FAB-MS (NBA matrix) m/z = 886.8 ($C_{32}H_{26}N_6RhP_2F_6^+$ requires 887.05).

Bisrhodium(III) 5,15-Bis[4-(4'-phenyl-2,2':6',2''-terpyridine)]-3,7,13,17-tetraethyl-2,8,12,18-tetramethyl Zinc Porphyrin Bis(4'-tolyl-2,2':6',2''-terpyridine) 6+ Series 14. Rhodium tolylterpyridine trichloride[25] (49 mg, 0.092 mmol) and silver tetrafluoroborate (59 mg, 0.3 mmol) were heated to reflux in 95 mL of an acetone/butanol (80/15) mixture under argon for 3 h. The reaction mixture was cooled to room temperature and filtered, and the precipitate of AgCl was washed with acetone. Butanol (35 mL) was added to the filtrate, and the acetone was pumped off. Bisterpyridineporphyrin **6** (50 mg, 0.046 mmol) was added to this solution, and the mixture was refluxed under argon for 8 h. The crude reaction mixture was cooled to room temperature and filtered. The precipitate obtained was washed with ethanol and dichloromethane and dissolved in acetonitrile. Anion exchange led to formation of a brown solid. Metalation of the porphyrin was carried out on the crude solid product using zinc acetate dihydrate (40 mg, 0.182 mmol) in 20 mL of an absolute methanol/acetonitrile mixture. The initial green-brown solution immediately turned red and was refluxed under argon for 1 h. The reaction mixture was cooled to room temperature before being subjected to anion exchange. The crude material was purified by repeated chromatography on silica gel with elution via an acetonitrile/water (9/1) mixture in which increasing amounts of saturated aqueous KNO_3 solution (maximum 1.5%) were added. After anion exchange, 66 mg (50% yield) of pure **14** was obtained: ^{1}H NMR (400 MHz, CD_3CN) δ = 10.31 (s, 2H), 9.50 (s, 4H), 9.14 (s, 4H), 8.95 (d, d, 4H, J = 8.1 and 0.7 Hz), 8.82 (d, d, 4H, J = 8.1 and 0.7 Hz), 8.69 (d, 4H, J = 8.2 Hz), 8.56 (d, 4H, J = 8.1 Hz), 8.39 (d, d, d, 4H, J = 7.9, 7.9, and 1.3 Hz), 8.37 (d, d, d, 4H, J = 7.9, 7.9, and 1.3 Hz), 8.19 (d, 4H, J = 8.1 Hz), 7.92 (m, 4H), 7.82 (d, 4H, J = 5.7 Hz), 7.66 (d, 4H, J = 7.8 Hz), 7.62 (d, d, d, 4H, J = 7.3, 5.8, and 1.3 Hz), 7.58 (d, d, d, 4H, J = 7.4, 5.9, and 1.3 Hz), 4.12 (q, 8H, J = 7.3 Hz), 2.67 (s, 12H), 2.59 (s, 6H), 1.85 (t, 12H, J = 7.5 Hz); mp > 300 °C ES-MS m/z = 335.15 ($C_{118}H_{96}N_{16}ZnRh_2^{6+}$ requires 335.23); UV-vis, (CH_3CN) λ_{max} (nm) 428, 546, 580.

Bisruthenium(II) 3,15-Bis-4-(4'-phenyl-2,2':6',2''-terpyridyl)-3,7,13,17-tetraethyl-2,8,12,18-tetramethyl Zinc Porphyrin Bis(4'-tolyl-2,2':6',2''-terpyridine) 6+ Series 13. This compound was prepared by analogy to **14** with the same solvents and the same quantities but with ruthenium tolylterpyridine trichloride[21] (68 mg, 0.13 mmol), $AgBF_4$ (83 mg, 0.426 mmol), and **6** (70 mg, 0.064 mol). Chromatography of the crude material was performed on silica gel with an acetone/water/aqueous saturated KNO_3 (90/10/0.07) mixture as eluent. After anion exchange, 80 mg (50%) of pure free-base porphyrin-derived material was obtained. The free-base porphyrin was metalated with zinc acetate dihydrate in 93% yield according to the procedure used for compounds **12** and **14**. Purification was performed on a silica gel column with the same eluent as for the corresponding free-base porphyrin compound: ^{1}H NMR (400 MHz, CD_3CN) δ = 10.31 (s, 2H), 9.41 (s, 4H), 9.05 (s, 4H), 8.84 (d, 4H, J = 8.2 Hz), 8.70 (d, 4H, J = 8.2 Hz), 8.68 (d, 4H, J = 8.2 Hz), 8.51 (d, 4H, J = 8.0 hz), 8.15 (d, 4H, J = 8.0 Hz), 8.04 (d, d, d, 4H, J = 7.1, 7.1, and 1.4 Hz), 8.01 (d, d, d, 4H, J = 7.8, 7.8, and 1.4 Hz), 7.62 (m, 4H), 7.60 (m, 4H), 7.52 (d, d, 4H, J = 5.7 and 0.8 Hz), 7.29 (d, d, d, 4H, J = 7.2, 5.9, and 1.2 Hz), 7.25 (d, d, d, 4H, J = 7.1, 6.0, and 1.2 Hz), 4.13 (q, 8H, J = 6.7 Hz), 2.70 (s, 12H), 2.57 (s, 6H), 1.86 (t, 12H, J = 7.5 Hz); mp > 300 °C; ES-MS m/z = 501.47 ($C_{118}H_{96}N_{16}Ru_2Zn^{4+}$ requires 501.38); UV-vis (CH_3CN) λ_{max} (nm) 429, 493, 543, 580.

Instrumentation. ^{1}H NMR spectra were recorded with a Bruker WP 200 SY or an AM 400 spectrometer. Chemical shifts are reported referenced to tetramethylsilane as an internal standard. Mass spectra were recorded on a Thomson TMN 208 (chemical ionization) or a VG ZAB-HF (FAB) spectrometer. The ground-state absorption spectra were recorded with either a Kontron Uvikon 860 or a Hitachi U3210 spectrophotometer. Luminescence spectra were recorded with a fully corrected Perkin-Elmer LS5 spectrofluorimeter. Melting points were determined on a Büchi SMP20 apparatus and were uncorrected. Cyclic voltammetry was carried out on a Bruker EI310 M potentiostat connected to an Ifelec 3802 XY recorder with a three-electrode system—either a Pt or a hanging mercury drop electrode as working electrode, a Pt-wire coil as auxiliary electrode, and a potassium chloride saturated calomel electrode (SCE) as reference were used. The reference electrode was separated from the bulk of the solution by a glass tube fitted on the bottom with a fine porosity sintered glass immersed in an acetonitrile solution containing tetra-*N*-butylammonium tetrafluoroborate (0.1 M). Experiments were carried out at 22 °C in acetonitrile solution (supporting electrolyte was 0.1 M tetra-*N*-butylammonium tetrafluoroborate) previously deoxygenated by purging for 20 min with high purity argon. Potentials are reported versus SCE. The sweep rate was 100 mV s^{-1}, and the experimental uncertainty was ±5 mV.

Luminescence lifetimes were measured by time-correlated, single-photon counting techniques using a mode-locked, synchronously pumped, cavity-dumped dye laser. The pump source was a frequency-doubled Antares 76S Nd:YAG laser equipped with an energy and spatial stabilizer. Rhodamine 6G and (frequency-doubled) Styryl-9 dye lasers were used to provide appropriate excitation wavelengths. Emission was isolated from scattered laser light using glass cutoff filters in conjunction with a high radiance monochromator, and decay profiles were recorded at six

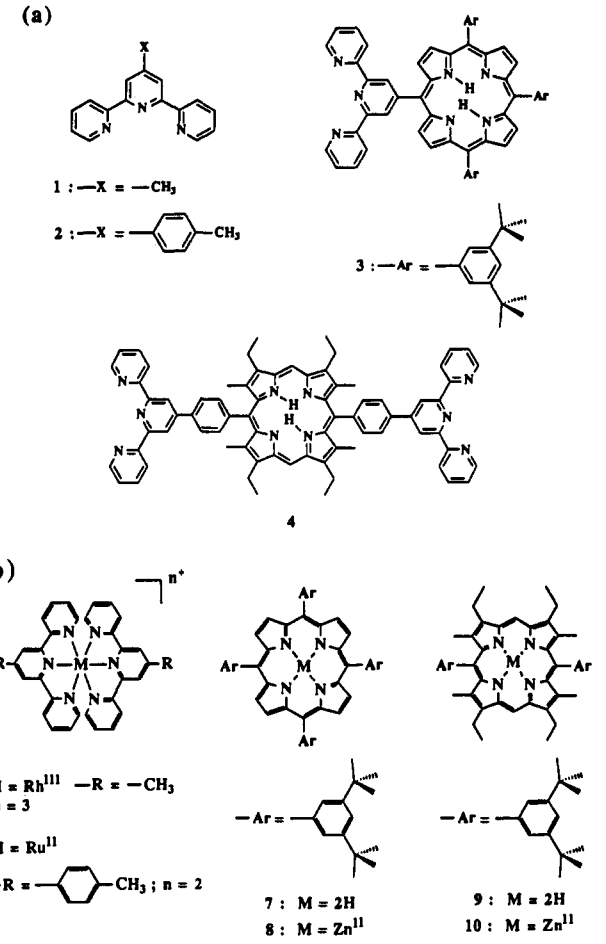

Figure 1. (a) Structures of the various substituted terpyridyl ligands and terpyridylporphyrin conjugates used in the present work. (b) Structures of the various reference complexes and porphyrins.

distinct wavelengths within the emission band. After deconvolution of the instrument response function (FWHM = 50 ps) and applying global analysis methodology, the time resolution of this instrument was about 15 ps.

Laser flash photolysis studies were made using a mode-locked, frequency-doubled Antares 76S Nd:YAG laser as the excitation pump for a Coherent Model 700 pyromethene dual-jet dye laser or a purpose-built styryl-9 dual-jet dye laser. A Quantel Model RGA67-10 regenerative amplifier, a Quantel Model PTA-60 dye laser, and a Continuum Model SPA1 autocorrelator were used to produce pulses of around 2 mJ with FWHM of about 300 fs. The spectrometer was run at 10 Hz, and the output pulse was split to produce excitation and monitoring pulses. Output from the pyromethene dye laser was at 586 nm, while output from the Styryl-9 dye laser was frequency-doubled to produce pulses at 430 nm (ca. 350 μJ). The monitoring pulse was delayed with a computerized optical delay stage, and spectra were acquired with a Princeton dual diode array spectrograph. About 600 individual laser shots were averaged for each time delay, and kinetic profiles were constructed by overlaying spectra collected at about 50 different delay times. Kinetic profiles were analyzed by nonlinear least-squares iteration using global analysis methodology.

Results and Discussion

Synthesis of the Ligands. The ligands used in the preparation of the porphyrin–metal bisterpyridine conjugates and the reference compounds are shown in Figure 1. Tolylterpyridine **2** was prepared according to the one-pot Hantzsch procedure developed by Case[28] and Calzaferri[29] and modified by Collin *et al.*[21] Although the preparation of methylterpyridine **1** is well documented,[30] we developed a new route which gives high yield (87%) and large amounts (10 g) of this compound (Scheme 1). This alternate route to methylterpyridine **1** involves the reaction of triflate terpyridine with tetramethyltin, using the general procedure described by Stille.[31] The triflate[22] was readily prepared in 67% overall yield in three steps from ethyl 2-pyridinecarboxylate and acetone.

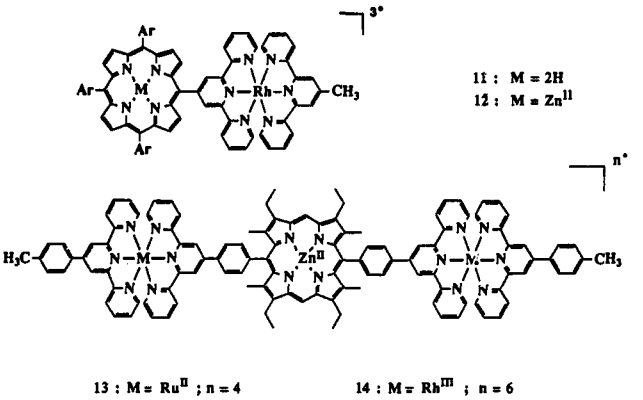

Figure 2. The various terpyridyl–porphyrin complexes studied here; conjugates **11** and **12** are dipartite systems, while the ruthenium and rhodium complexes **13** and **14** are tripartite conjugates.

Scheme 1

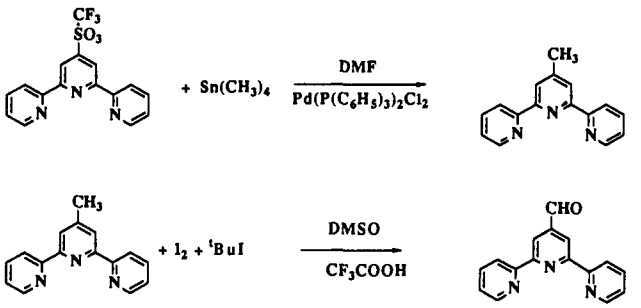

Synthesis of a porphyrin bearing a terpyridine residue requires access to a terpyridine possessing an aldehyde group. A Sommelet reaction applied to tolylterpyridine **2** led to the corresponding aldehyde in 40% yield, whereas formylterpyridine was prepared from **1** by a modified procedure as developed by Vismara *et al.*[32] A mixture of *tert*-butyl iodide, iodine, trifluoroacetic acid, and methylterpyridine **1** in dimethyl sulfoxide yields both formylterpyridine and terpyridinecarboxylic acid. The monoterpyridine porphyrin **3** was prepared following Adler's procedure,[33] and the symmetrical reference porphyrin **7** was also obtained as a byproduct of this reaction. Extensive chromatography was required to obtain pure **3**, which was isolated in 7% yield.

The synthetic strategy for the preparation of bisterpyridine porphyrin **4** derives from MacDonald's methodology,[34] using the improved procedure developed by Lindsey *et al.*[35] Since the dipyrrylmethane[24] precursor is subject to decomposition, it was prepared from the diester shortly before use. The ligand **4** was obtained pure in 42% yield after two recrystallizations of the crude material.

(28) Case, F. H.; Kaspen, T. J. *J. Am. Chem. Soc.* **1956**, *78*, 5842.
(29) Spahni, W.; Calzaferri, G. *Helv. Chim. Acta* **1984**, *67*, 450.
(30) (a) Bates, R. B.; Gordon, B.; Keller, P. C.; Rund, J. V.; Mills, N. S. *J. Org. Chem.* **1980**, *45*, 168. (b) Bell, T. W.; Hu, L. Y. *Tetrahedron Lett.* **1988**, *29*, 4819. (c) Potts, K. T.; Usifer, D. A.; Guadalupe, A.; Abruna, H. D. *J. Am. Chem. Soc.* **1987**, *109*, 3961.
(31) Echararren, A. M.; Stille, J. K. *J. Am. Chem. Soc.* **1987**, *109*, 5478.
(32) Vismara, E.; Fontana, F.; Minisci, F. *Gazz. Chim. Ital.* **1987**, *117*, 135.
(33) Adler, A. D.; Longo, F. R.; Finarelli, J. D.; Goldmacher, J.; Assour, J.; Korsakoff, L. *J. Org. Chem.* **1967**, *32*, 476.
(34) Arsenault, G. P.; Bullock, E.; MacDonald, S. F. *J. Am. Chem. Soc.* **1960**, *82*, 4384.
(35) Lindsey, J. S.; Schreiman, J. C.; Hsu, H. C.; Kearney, P. C.; Marguerattaz, A. M. *J. Org. Chem.* **1987**, *52*, 827.

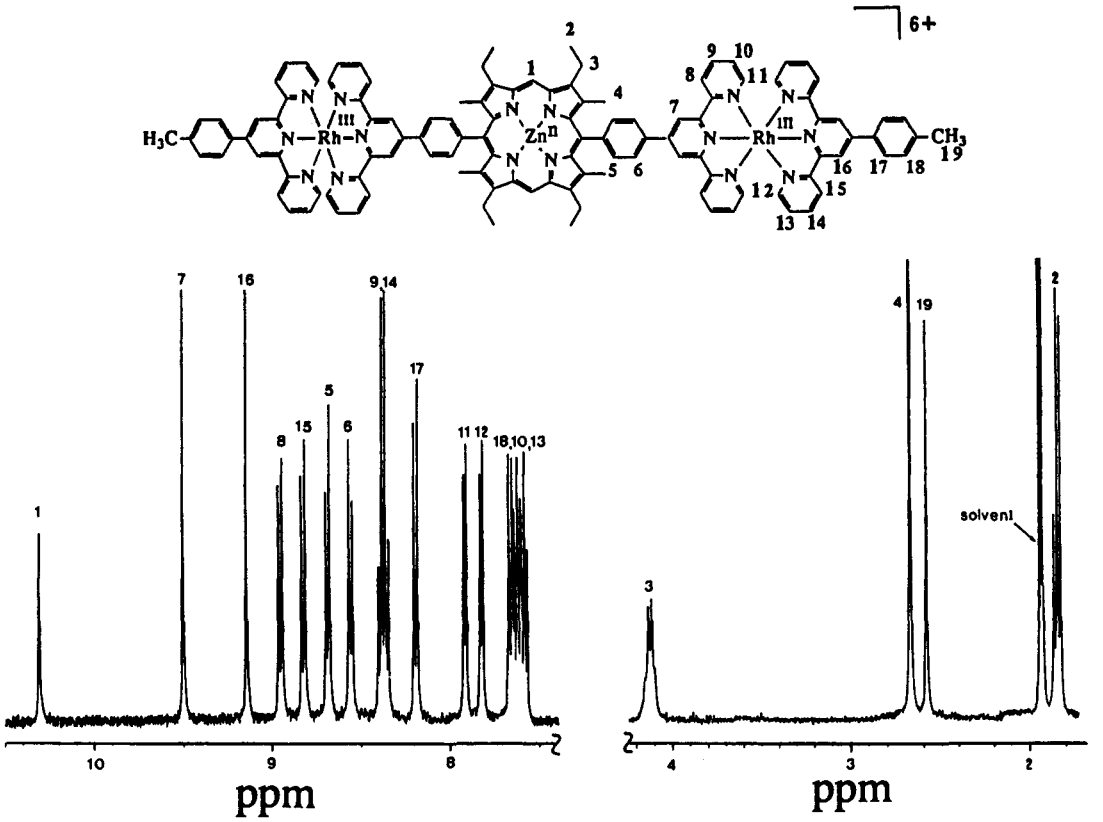

Figure 3. ^{1}H NMR spectrum (CD_3CN, 400 MHz) of **14** with numbering of the various protons in the chemical formula and complete assignment.

Synthesis of the Complexes. Structures for the various complexes synthesized here are shown in Figure 2. The rhodium(III) and ruthenium(II) complexes were prepared following the same strategy. In the first step, a given substituted terpyridine **1** or **2** was reacted with the metal trichloride according to literature procedures[21,24] and yielded $MLCl_3$ (M = Ru^{III} or Rh^{III}; L = **1** or **2**). In the second step, after dechlorination with silver tetrafluoroborate, the solvated complex $ML(acetone)_3^{n+}$ (M = Ru^{III} or Rh^{III}; L = **1** or **2**) was reacted with the appropriate substituted terpyridine (**1**, **2**, **3**, or **4**) in refluxing alcohol (ethanol or 1-butanol). This method was particularly suitable for the preparation of asymmetrical bisterpyridine–metal complexes and was also useful for the preparation, in good yield, of symmetrical compounds such as **13** and **14**.

Metalation of a porphyrin with zinc(II) acetate for compounds **8**, **10**, **12**, **13**, and **14** was almost quantitative. After chromatography and anion exchange, the purity of each highly colored complex was checked by thin-layer chromatography, UV–visible spectroscopy, high-resolution ^{1}H NMR spectrometry, and mass spectroscopy. The ^{1}H NMR spectrum of **14** (400 MHz) is given in Figure 3 as an example.

Photophysical Properties of the Individual Components. The photophysical and electrochemical properties of the isolated porphyrins **7**–**10** have been reported previously.[36,37] The rhodium(III)–bisterpyridyl complex **5** does not emit in fluid solution at room temperature but displays a long-lived (i.e., $\tau_p \approx 10$ μs) phosphorescence centered at 720 nm in an ethanol glass at 77 K. The observed spectrum was in good accord with that reported previously by Ford *et al.*,[38] who estimated a triplet energy of 2.28 eV by analyzing the spectrum according to a Gaussian band shape. This emission has been attributed to the lowest energy triplet ligand field state.[38] The triplet state can also be detected by laser flash photolysis methods in deoxygenated ethanol at room temperature, and the derived transient absorption spectrum is shown as Figure 4a. The spectrum is very weak and structureless with a maximum around 390 nm. Under these conditions, the triplet decays with a lifetime of *ca.* 4 ns and is formed within the laser pulse (i.e., <500 fs) (Figure 4b).

The ruthenium(II)–bisterpyridyl complex **6** shows extremely weak luminescence in acetonitrile solution at room temperature with a maximum at 650 nm. This corresponds to a triplet energy of *ca.* 1.90 eV. The luminescence quantum yield was determined to be less than 0.0002, while the lifetime, measured by time-correlated, single-photon counting techniques, was (565 ± 35) ps. Emission is attributed to the lowest energy metal-to-ligand charge-transfer state.[39] This species can also be detected by laser flash photolysis methods, and the observed transient differential absorption spectrum is provided as Figure 5a. In addition to bleaching of the intense ground-state absorption band centered at 450 nm, the spectrum shows strong absorption at both higher and lower energies. The signal decayed cleanly the the prepulse baseline by first-order kinetics with a lifetime of (610 ± 40) ps (Figure 5b).

On the basis of these luminescence studies, triplet energy transfer is calculated to be energetically favorable from the rhodium(III)– and ruthenium(II)–bisterpyridyl complexes to each of the porphyrins. Such processes are considered important since they provide an antenna effect in which light not absorbed directly by the porphyrin can still be used to initiate electron transfer. In contrast, singlet energy transfer from a porphyrin to a bisterpyridyl complex is energetically unfavorable in all cases, and such reactions do not represent viable routes for quenching of porphyrin excited singlet states.

Electrochemistry of the Multicomponent Systems. Cyclic voltammetry studies were made with the various monomeric and multinuclear complexes in dichloromethane or acetonitrile solution. Following from the studies carried out with the monomers,

(36) Brun, A. M.; Harriman, A.; Heitz, V.; Sauvage, J.-P. *J. Am. Chem. Soc.* **1991**, *113*, 8657.

(37) Chambron, J.-C.; Harriman, A.; Heitz, V.; Sauvage, J.-P. *J. Am. Chem. Soc.* **1993**, *115*, 6109.

(38) Frink, M. E.; Sprouse, S. D.; Goodwin, H. A.; Watts, R. J.; Ford, P. C. *Inorg. Chem.* **1988**, *27*, 1283.

(39) Kirchoff, J. R.; McMillin, D. R.; Marnot, P. A.; Sauvage, J.-P. *J. Am. Chem. Soc.* **1985**, *107*, 1138.

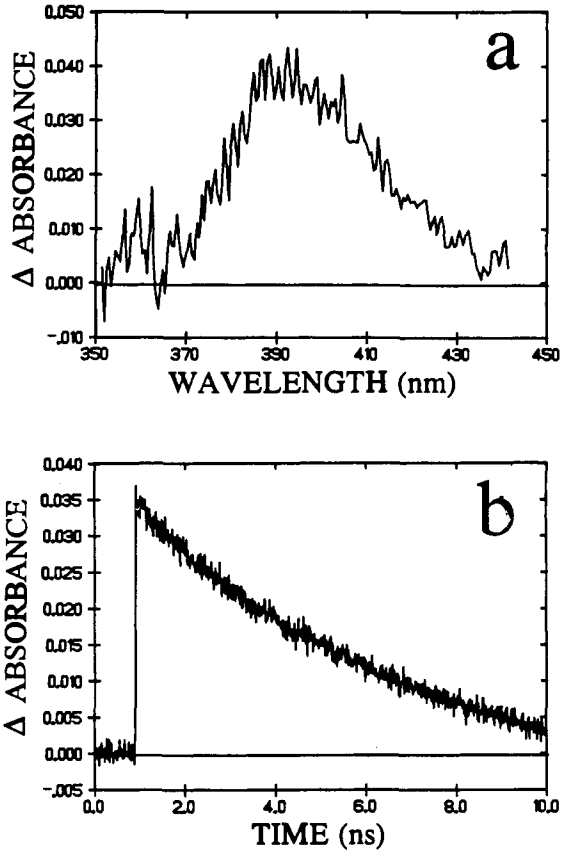

Figure 4. (a) Differential transient absorption spectrum recorded 200 ps after laser excitation of the rhodium(III)–bisterpyridyl complex **5** in acetonitrile solution. (b) Kinetic trace recorded at 400 nm for the above experiment showing decay of the triplet to the ground state.

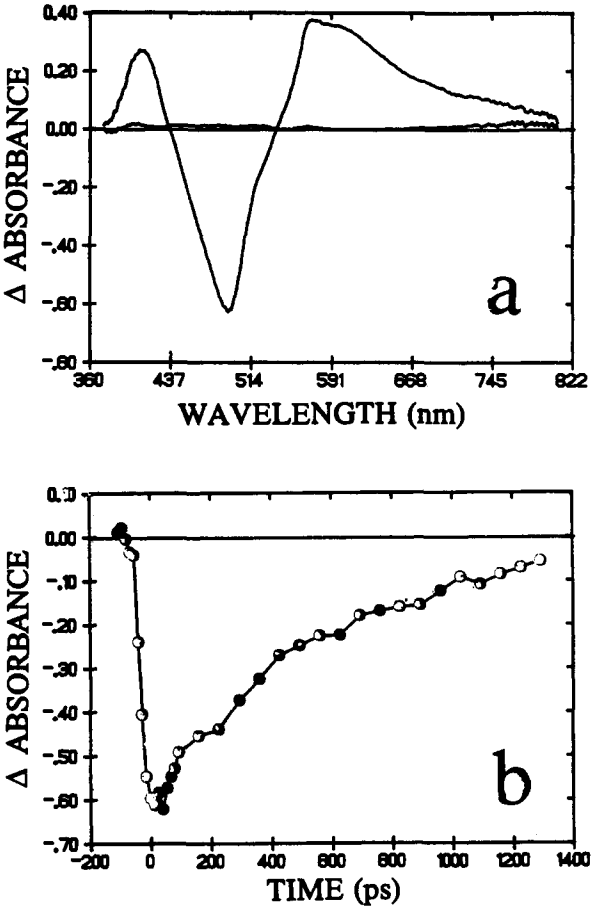

Figure 5. (a) Differential transient absorption spectrum recorded 30 ps after laser excitation of the ruthenium(II)–bisterpyridyl complex **6** in acetonitrile solution. (b) Kinetic trace recorded at 500 nm for the above experiment showing restoration of the ground state.

it is clear that for the multinuclear complexes the most readily oxidized subunit is the porphyrin ring, while addition of an electron occurs at the metal–bisterpyridyl complex. Redox potentials measured for removal of one ($E_{ox}[1]$) or two ($E_{ox}[2]$) electrons and for addition of one ($E_{red}[1]$) or two ($E_{red}[2]$) electrons are compiled in Table 1 for both monomeric and multinuclear complexes. The derived values were used in conjunction with excited-state energy levels determined by luminescence spectroscopy to derive the reaction exergonicities for photoinduced electron transfer following selective excitation of the multinuclear complexes.[40] The reported values were not corrected for changes in electrostatic potentials that accompany electron transfer. Within this restriction, it was concluded that photoinduced electron transfer from the first excited singlet state of a porphyrin to an appended metal–bisterpyridyl complex is exergonic, in each case (Table 2). The corresponding reactions involving electron abstraction by the first excited singlet state of the porphyrin were found to be endergonic, in each case, as were the reactions involving electron donation to or abstraction by the triplet excited state of the ruthenium(II)–bisterpyridyl complex. Photoinduced electron abstraction from the appended zinc porphyrin by the triplet excited state of the rhodium(III)–bisterpyridyl complex is also predicted to be thermodynamically favorable. On this basis, the most probable photoinduced electron-transfer reactions involve reduction of the appended metal–bisterpyridyl complex by the excited singlet state of the porphyrin or *via* the triplet state of the rhodium(III) complex.

Photochemistry of the Zinc Porphyrin–Ruthenium–Bisterpyridyl Conjugate 13. The absorption spectrum recorded for **13** in acetonitrile solution (Figure 6a) appears to be an exact superposition of spectra recorded for the monomeric components

Table 1. Redox Potentials (in V vs SCE) Measured by Cyclic Voltammetry for the Various Monomeric Models and the Binuclear Compounds

compound	solvent	$E_{ox}[1]$	$E_{ox}[2]$	$E_{red}[1]$	$E_{red}[2]$
13	CH_3CN	0.66	0.82	−1.24	−1.47
14	CH_3CN	0.66	0.88	−0.59[b]	
12	CH_3CN	0.74	1.31	−0.62[b]	−1.40
11	CH_3CN	1.09		−0.62[b]	−1.05
8	DMF[a]	0.62	0.90	−1.63	−1.85
7	CH_2Cl_2	1.07	1.32	−1.09	−1.43
10	DMF[a]	0.64	0.95	−1.60	−1.83
5	CH_3CN			−0.60[b]	
6	CH_3CN	1.25		−1.24	−1.47

[a] *N,N*-Dimethylformamide. [b] Irreversible.

without perturbation of the respective electronic systems. Thus, the two subunits appear to be electronically remote. Excitation of **13** in acetonitrile solution at 586 nm, where only the zinc porphyrin subunit absorbs, resulted in detection of extremely weak fluorescence ($\Phi_f < 0.0005$) relative to that observed ($\Phi_f = 0.04$) for an optically matched 2:1 molar mixture of **6** and **10** in acetonitrile. Time-resolved fluorescence studies indicated that the lifetime of the excited singlet state of the zinc porphyrin subunit in **13** was (26 ± 5) ps, compared to a value of (2.2 ± 0.1) ns observed for the corresponding monomeric porphyrin **10**. The characteristic transient differential absorption spectrum of the zinc porphyrin excited singlet state[41] was observed immediately after excitation of **13** with a 0.3-ps laser pulse at 586 nm (Figure 7a). This species decayed rapidly, with a lifetime of (30 ± 5) ps, to generate a long-lived transient species which exhibited

(40) Calculated according to $\Delta G° = -F\{(E_{red}[1] - E_{ox}[1]) - E_{es}\}$ where E_{es} refers to the excitation energy of the chromophore.

(41) Rodriguez, J.; Kirmaier, C.; Holten, D. *J. Am. Chem. Soc.* **1989**, *111*, 6500.

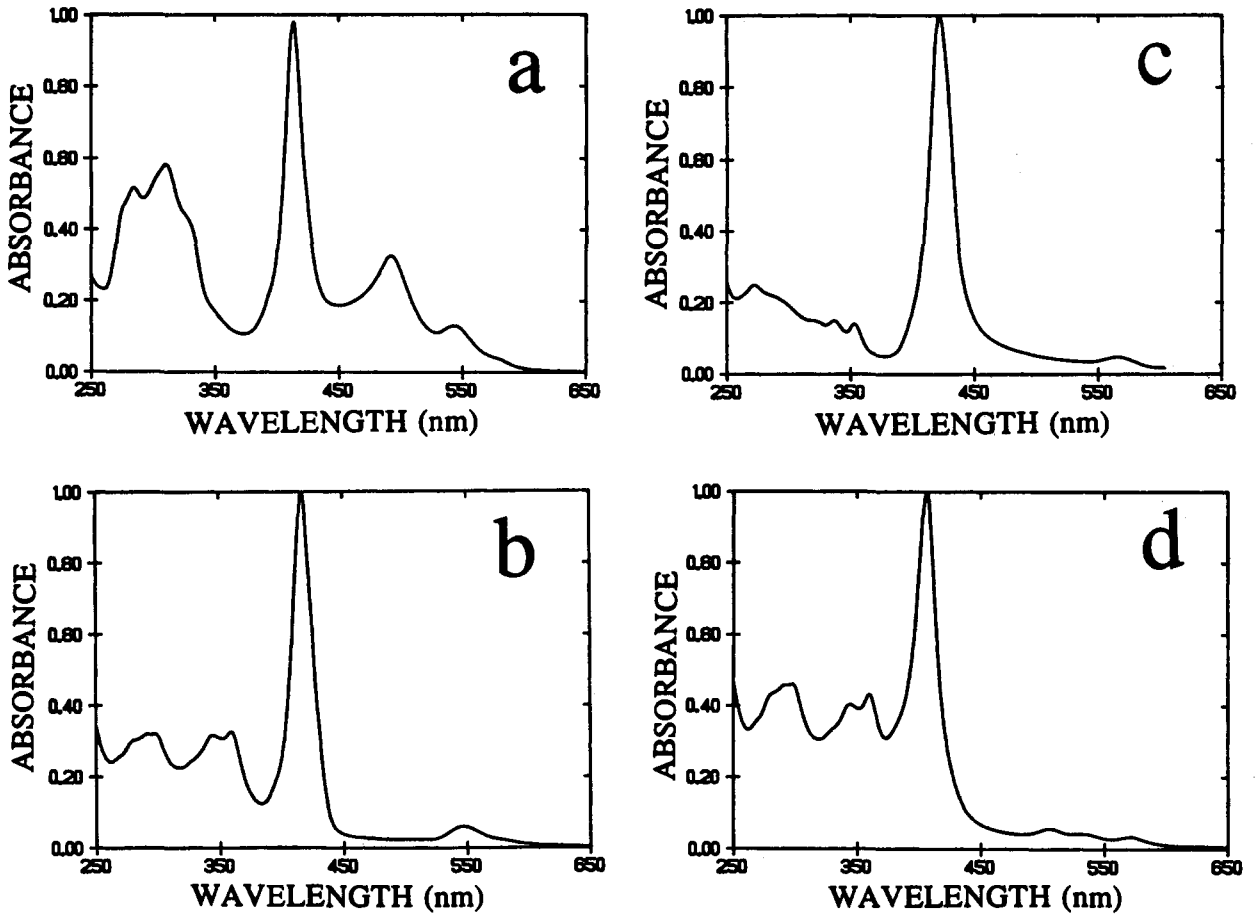

Figure 6. Absorption spectra recorded in dilute acetonitrile solution for (a) **13**, (b) **14**, (c) **12**, and (d) **11**.

Table 2. Reaction Exergonicities for the Various Photoinduced Electron-Transfer Processes Considered for the Multinuclear Compounds

compound	reaction	$\Delta G°$ (eV)
13	*(ZnP)-Ph-Ru(II) → ($^{\bullet+}$ZnP)-Ph-Ru(I)	−0.28
13	*(ZnP)-Ph-Ru(II) → ($^{\bullet-}$ZnP)-Ph-Ru(III)	+0.67
13	(ZnP)-Ph-Ru(II)* → ($^{\bullet+}$ZnP)-Ph-Ru(I)	+0.82
13	(ZnP)-Ph-Ru(II)* → ($^{\bullet-}$ZnP)-Ph-Ru(III)	0.00
14	*(ZnP)-Ph-Rh(III) → ($^{\bullet+}$ZnP)-Ph-Rh(II)	−0.71
14	(ZnP)-Ph-Rh(III)* → ($^{\bullet+}$ZnP)-Ph-Rh(II)	−0.81
12	*(ZnP)-Rh(III) → ($^{\bullet+}$ZnP)-Rh(II)	−0.58
12	(ZnP)-Rh(III)* → ($^{\bullet+}$ZnP)-Rh(II)	−0.80
11	*(H_2P)-Rh(III) → ($^{\bullet+}H_2$P)-Rh(II)	−0.19
11	(H_2P)-Rh(III)* → ($^{\bullet+}H_2$P)-Rh(II)	−0.57

significant absorption in the far-red region of the spectrum. This latter transient, which decayed with a lifetime of (2.0 ± 0.2) ns to reform the ground-state system (Figure 7b and c), is assigned to a mixture of the zinc porphyrin π-radical cation[42] and the corresponding ruthenium(I)–bisterpyridyl complex as formed by intramolecular electron transfer. [Note, the so-called ruthenium-(I)–bisterpyridyl complex is more correctly described as a ruthenium(II) bisterpyridyl π-radical anion.]

$$^{s*}\text{(ZnP)-Ph-Ru(II)} \xrightarrow[\Delta G° = -0.28\ \text{eV}]{} (^{\bullet+}\text{ZnP})\text{-Ph-Ru(I)} \quad (2)$$

$$(^{\bullet+}\text{ZnP})\text{-Ph-Ru(I)} \xrightarrow[\Delta G° = -1.90\ \text{eV}]{} \text{ZnP-Ph-Ru(II)} \quad (3)$$

On the basis of these measurements, the rate constants for forward (i.e., reaction 2) and reverse (i.e., reaction 3) electron-transfer steps, respectively, are (3.6 ± 0.4) × 10^{10} and (5.0 ± 0.5) × 10^{8} s^{-1}. The quantum yield for formation of the zinc porphyrin π-radical cation, as estimated from the transient absorption spectral changes, is *ca.* 100%. Unlike the systems possessing a directly coupled rhodium(III) complex (see later), the rate of reverse electron transfer is considerably slower than that of the forward reaction. This differential in rates of forward and reverse electron transfers may be qualitatively explained in terms of the Marcus "inverted effect" (see later).[43]

Excitation of **13** in acetonitrile solution at 430 nm, where only the ruthenium(II)–bisterpyridyl complex absorbs, resulted in detection of extremely weak luminescence with a spectral profile similar to that observed for the monomeric ruthenium(II) complex **6**. From time-correlated, single-photon counting studies the luminescence lifetime was found to be (240 ± 30) ps, compared to a value of (565 ± 35) ps recorded for **6**. Flash photolysis studies, following excitation of **13** with a 0.3-ps laser pulse at 430 nm, showed that the excited triplet state of the ruthenium(II) complex was present immediately after the excitation pulse (Figure 8a). This species decayed rapidly to form the triplet excited state of the zinc porphyrin. The latter species was observed to be formed with a first-order rate consetant of (3.5 ± 0.7) × 10^{9} s^{-1}, by monitoring growth of the porphyrin triplet at 440 nm (Figure 8b). These observations are consistent with rapid intramolecular triplet energy transfer, for which the averaged rate constant is (3 ± 1) × 10^{9} s^{-1}.

$$\text{ZnP-Ph-(Ru(II))}^{*t} \xrightarrow[\Delta E = 0.15\ \text{eV}]{} {}^{t*}\text{(ZnP)-Ph-Ru(II)} \quad (4)$$

The triplet energy gap, estimated from low-temperature phosphorescence spectra, is 0.15 eV, and this should be sufficient to ensure irreversible energy transfer.

Intramolecular triplet energy transfer may occur by way of

(42) Carnieri, N.; Harriman, A. *Inorg. Chim. Acta* **1982**, *62*, 103.

(43) Marcus, R. A. *Discuss. Faraday Soc.* **1960**, *29*, 21.

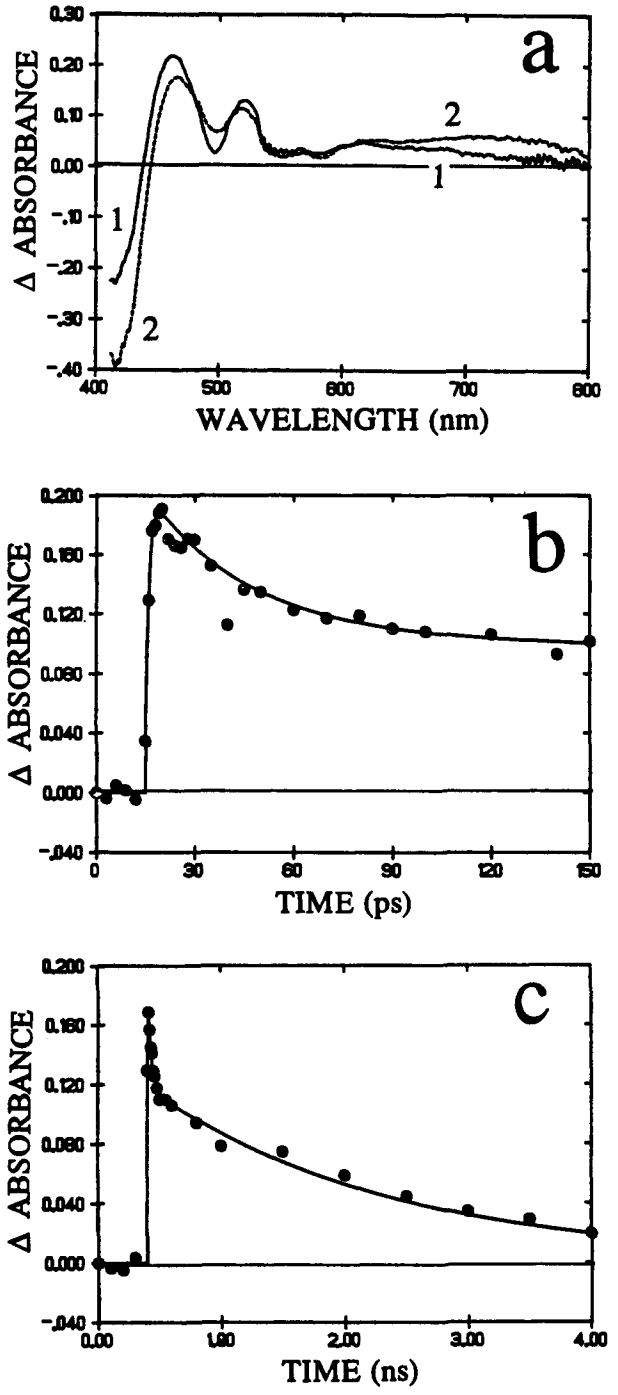

Figure 7. (a) Differential transient absorption spectra recorded (1) 1 and (2) 200 ps after excitation of **13** in acetonitrile solution with a 0.3-ps laser pulse at 586 nm. (b) and (c) Kinetic traces showing decay of the transient species at 470 nm for the above experiment as recorded over different time scales.

Förster or Dexter mechanisms. For Förster-type energy transfer,[44] the overlap intergral (J_F) was determined to be 1.6×10^{-15} mmol cm^6

$$J_F = \frac{\int F(\nu)\epsilon(\nu)\nu^{-4}\,d\nu}{\int F(\nu)d\nu} \qquad (5)$$

where $F(\nu)$ is the luminescence intensity at wavenumber ν (in cm^{-1}), and $\epsilon(\nu)$ is the molar extinction coefficient of the porphyrin subunit (in cm^{-1} M^{-1}), with only the Q-transitions being

(44) Förster, T. *Discuss. Faraday Soc.* **1959**, *27*, 7.

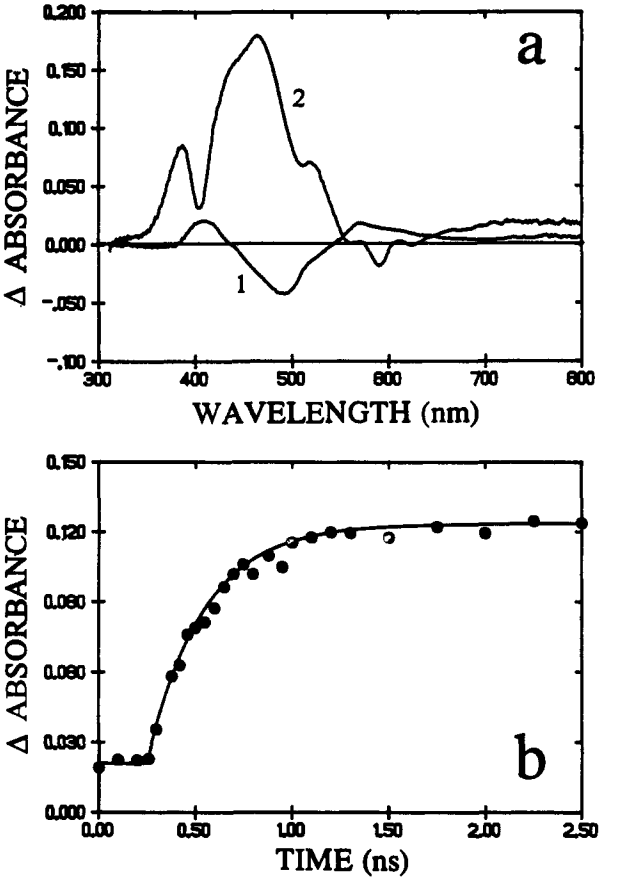

Figure 8. (a) Differential transient absorption spectra recorded (1) 10 ps and (2) 2 ns after excitation of **13** in acetonitrile solution with a 0.3-ps laser pulse at 430 nm. (b) Kinetic trace showing formation of the zinc porphyrin triplet excited state at 440 nm (an isosbestic point for the triplet state of the ruthenium(II) complex) due to intramolecular triplet energy transfer.

considered. Using this value together with the photophysical data derived for the monomeric ruthenium(II) complex **6**, the reciprocal of the rate constant for intramolecular triplet energy transfer in the multinuclear compound **13** (τ_F) was calculated to be 130 ns. This determination was made on the basis of the following expression:[44]

$$\tau_F^{-1} = \frac{8.8 \times 10^{-25} K^2 \Phi_L J_F}{n^4 \tau R^6} \qquad (6)$$

Here, K is a factor that describes the mutual orientation of the two subunits ($K = 1$), n is the solvent refractive index, and the center-to-center separation distance (R) was estimated to be 15 Å from space-filling molecular models. The derived τ_F is very much longer than the experimental value of 330 ps, but it should be noted that the R^{-6} dependence might be inappropriate for closely coupled chromophores.[45] However, following from the calculations of Kenkre and Knox[46] and using a value for the electronic matrix coupling element (V) derived from analysis of the data according to a Dexter mechanism (see below; $V = 22$ cm^{-1}), we would expect the R^{-6} dependence to hold for this system. Thus, triplet energy transfer by the Förster mechanism appears unlikely in this case.

For photon migration via the Dexter mechanism,[47] the overlap integral (J_D) was determined to be 5×10^{-6} cm using the following expression:

(45) Jean, J. M.; Chan, C.-K.; Fleming, G. R. *Isr. J. Chem.* **1988**, *28*, 169.
(46) Kenkre, V. M.; Knox, R. S. *Phys. Rev. Lett.* **1974**, *33*, 803.
(47) Dexter, D. L. *J. Chem. Phys.* **1953**, *21*, 836.

$$J_D = \frac{\int F(\nu)\epsilon(\nu)d\nu}{\int F(\nu)d\nu \int \epsilon(\nu)d\nu} \quad (7)$$

To account for the observed transfer time (τ_D) of 330 ps, the electronic matrix coupling element V would have to correspond to 22 cm^{-1} for triplet energy transfer to occur by way of a Dexter mechanism.[48]

$$\tau_D^{-1} = \frac{4\pi^2 V^2 J_D}{h} \quad (8)$$

This seems to be a reasonable estimate for V, given the separation distance, and it should be recalled that triplet energy transfer by the Dexter mechanism corresponds to a double electron transfer involving both LUMO and HOMO sites on the reactants.

Photochemistry of the Phenyl-Linked Zinc Porphyrin–Rhodium–Bisterpyridyl Conjugate 14. The absorption spectrum recorded for **14** closely resembled a superposition of spectra of the individual components (Figure 6b), but fluorescence from the zinc porphyrin subunit could not be detected upon excitation at 586 nm. Furthermore, porphyrin fluorescence could not be resolved from the instrumental response function during time-correlated, single-photon counting studies such that the lifetime must be <15 ps. Flash photolysis studies carried out with **14** in acetonitrile solution showed that the porphyrin excited singlet state was present immediately after excitation with a 0.3-ps laser pulse at 586 nm (Figure 9a). This species decayed with a lifetime of only (3.1 ± 0.4) ps to leave a longer lived residual transient species. The latter species decayed to restore the ground-state system with a lifetime of (120 ± 10) ps and is attributed to a mixture of the zinc porphyrin π-radical cation and the corresponding rhodium-(II) complex (Figure 9b,c). [Note, the so-called rhodium(II)–bisterpyridyl complex may be better described as a rhodium(III) bisterpyridyl π-radical anion.]

$$^{s*}(ZnP)\text{-}Ph\text{-}Rh(III) \xrightarrow[\Delta G^\circ = -0.71\ eV]{} (^{\bullet+}ZnP)\text{-}Ph\text{-}Rh(II) \quad (9)$$

$$(^{\bullet+}ZnP)\text{-}Ph\text{-}Rh(II) \xrightarrow[\Delta G^\circ = -1.47\ eV]{} ZnP\text{-}Ph\text{-}Rh(III) \quad (10)$$

As above, the quantum yield for formation of the zinc porphyrin π-radical cation approaches 100%. The rates of both forward ($k_9 = 3.2 \times 10^{11}\ s^{-1}$) and reverse ($k_{10} = 8.3 \times 10^9\ s^{-1}$) electron-transfer processes are significantly faster for the rhodium(III)-containing tripartite compound than those found for the corresponding ruthenium(II) counterpart, while, in both cases, the rate of reverse electron transfer is much slower than that for the forward step. These observations may be explained in terms of the energy gap law. Thus, the rate constant for a nonadiabatic electron-transfer process (k) can be described as the product of the square of the electronic matrix coupling element (V) and the Franck–Condon weighted density of states (FCWD):[49]

$$k = (4\pi^2/h)V^2[FCWD] \quad (11)$$

The FCWD can be evaluated using the quantum mechanical correction introduced by Jortner *et al.*[50] so that k can be expressed in terms of the reaction exergonicity (ΔG°). As can be seen from Figure 10, the rate constants derived for **13** and **14** are well described in terms of eq 11 with V = 35 cm^{-1}. The total reorganization energy (λ) for the phenyl-bridged tripartite compounds was derived to be 6300 cm^{-1} (i.e., 0.78 eV), following evaluation of the FCWD term. Although these parameters are far from unique solutions to eq 11, the derived estimates for both V and λ seem to be realistic. Indeed, V is comparable to values

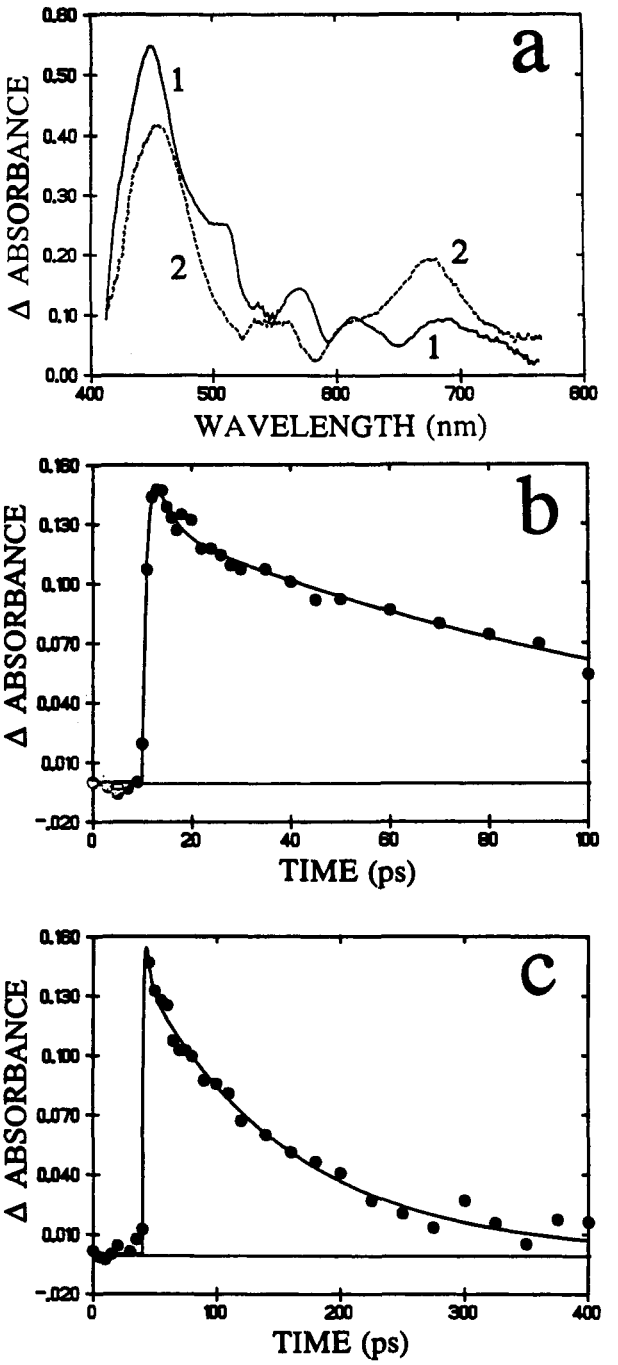

Figure 9. (a) Differential transient absorption spectra recorded (1) 1 and (2) 100 ps after excitation of **14** in acetonitrile solution with a 0.3-ps laser pulse at 586 nm. (b) and (c) Kinetic traces showing decay of the transient species at 470 nm for the above experiment as recorded over different time scales.

derived for somewhat related bisporphyrins[36,37] and porphyrin-quinone compounds[51] and is in the same range as that found for triplet energy transfer in **13**. Also, we would expect to observe only a modest reorganization energy in view of the small edge-to-edge separation distance and the fact that oxidation of the zinc porphyrin is accompanied by negligible structural change.

Intramolecular triplet energy transfer from the rhodium(III)–bisterpyridyl complex to the porphyrin is calculated to be energetically favorable.

$$ZnP\text{-}Ph\text{-}(Rh(III))^{*t} \xrightarrow[\Delta E = 0.53\ eV]{} {}^{t*}(ZnP)\text{-}Ph\text{-}Rh(III) \quad (12)$$

However, the poor spectral profile, absence of room temperature

(48) Oevering, H.; Verhoeven, J. W.; Paddon-Row, M. N.; Cotsaris, E.; Hush, N. S. *Chem. Phys. Lett.* **1988**, *143*, 488.
(49) Rips, I.; Jortner, J. *J. Chem. Phys.* **1987**, *87*, 2090.
(50) Kestner, N. R.; Logan, J.; Jortner, J. *J. Phys. Chem.* **1974**, *78*, 2148.
(51) Wasielewski, M. R. *Chem. Rev.* **1992**, *92*, 435.

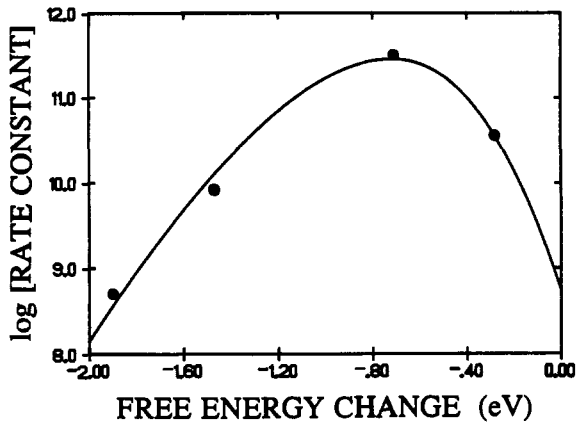

Figure 10. Dependence of the rate constant for electron transfer on the reaction exergonicity for the tripartite compounds **13** and **14** in acetonitrile solution. The solid line is a computed "best fit" to eq 11 with the parameters given in the text.

luminescence, and very weak triplet absorption spectrum characteristic of the rhodium chelate prevented meaningful study of this effect. Excitation of **14** with a 0.3-ps laser pulse at 298 nm, where the rhodium(III)–bisterpyridyl complex absorbs about 50% of incident light, did not result in significant population of the porphyrin triplet state. Although photoinduced electron abstraction by the triplet excited state of the rhodium(III) complex is expected to occur (Table 2), we were unable to resolve this effect from the photochemistry taking place following direct light absorption by the porphyrin chromophore.

Photochemistry of Directly Linked Porphyrin–Rhodium–Bisterpyridyl Conjugates 11 and 12. Absorption spectra recorded for the binuclear compounds **11** and **12** in acetonitrile solution resembled those found for equimolar mixtures of the individual components but were clearly distorted (Figure 6c,d). This may indicate some steric crowding due to the closely spaced subunits. Fluorescence could not be properly resolved from the background for the zinc analogue **12**, while the monomeric zinc porphyrin **8** fluoresces with moderate quantum yield (Φ_f = 0.045). Fluorescence from the free-base analogue **11** was extremely weak ($\Phi_f \approx 0.0001$) relative to that observed for the monomer **7** (Φ_f = 0.19). Time-resolved fluorescence studies, using time-correlated, single photon counting techniques with 15-ps temporal resolution, could not properly resolve the fluorescence profiles from the instrumental response function for either of the binuclear complexes. These studies indicate that the appended rhodium(III)–bisterpyridyl complex is an avid quencher for the porphyrin excited singlet state and that in the binuclear complexes the porphyrin fluorescence lifetimes are less than 15 ps.

Laser flash photolysis studies with excitation at 586 nm made with **11** and **12** in acetonitrile solution at room temperature showed that the excited singlet state of the porphyrin subunit was present immediately after the excitation pulse (Figures 11 and 12). In both cases, the excited singlet state decayed rapidly back to the ground state, apparently without generation of a long-lived intermediate. The decay profiles could be analyzed satisfactorily in terms of single-exponential processes, perhaps because of the limited precision of the experimental data (Figures 11 and 12). Under such conditions, the singlet excited-state lifetimes derived for the zinc porphyrin **12** and the free-base analogue **11**, respectively, were (0.7 ± 0.2) ps and (5.5 ± 0.5) ps. We attribute fluorescence quenching to intramolecular electron transfer followed by rapid reverse electron transfer, although the spectroscopic records do not support formation of long-lived redox products.

$$*(ZnP)\text{-}Rh(III) \xrightarrow[\Delta G^\circ = -0.58\ eV]{} (^{\bullet+}ZnP)\text{-}Rh(II) \xrightarrow[\Delta G^\circ = -1.48\ eV]{} ZnP\text{-}Rh(III) \quad (13)$$

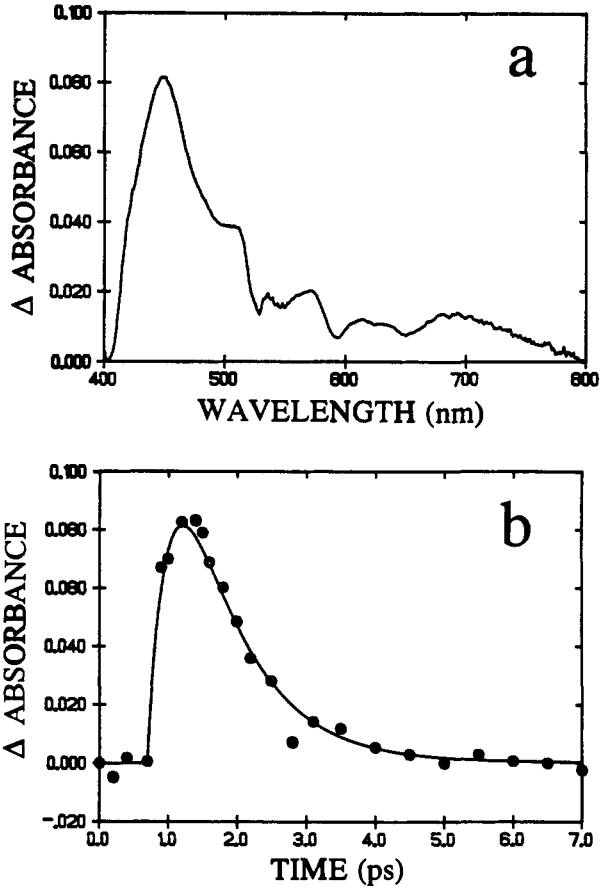

Figure 11. (a) Differential transient absorption spectra recorded 0.5 ps after excitation of **12** with a 0.3-ps laser pulse at 586 nm; the spectra are corrected for spectral chirp. (b) Kinetic trace showing decay of the transient species at 470 nm for the above experiment.

$$*(H_2P)\text{-}Rh(III) \xrightarrow[\Delta G^\circ = -0.19\ eV]{} (^{\bullet+}H_2P)\text{-}Rh(II) \xrightarrow[\Delta G^\circ = -1.71\ eV]{} H_2P\text{-}Rh(III) \quad (14)$$

Similar studies were made with the binuclear compounds in a few other polar solvents, and the results are collected in Table 3. It is seen that for the zinc porphyrin-based derivative **12** the lifetime of the excited singlet state is comparable to the reorientation time of the solvent (τ_L)[52] in the limited range of solvents that could be used. For the free-base porphyrin analogue **11**, the singlet lifetime is around 5 ps in rapidly relaxing solvents but increases in ethanol and, to a lesser extent, benzonitrile, which are characterized by considerably longer τ_L.

For solvents with fast τ_L, the derived rates of electron transfer can be approximated by the following expression:[53]

$$k \approx \alpha \exp[-\Delta G^*/k_B T] \quad (15a)$$

$$\alpha \approx (1/\tau_L) \quad (15b)$$

Assuming that reaction occurs within the adiabatic limit with internal vibrational modes being ignored, the frequency factor α can be set equal to the inverse of the solvent reorientation time. Under such restrictions, the averaged activation free energy

(52) The longitudinal relaxation time of the solvent $\tau_L = (\epsilon_\infty/\epsilon_S)\tau_D$ where ϵ_∞ is the optical dielectric constant, ϵ_S is the static dielectric constant, and τ_D is the Debye dielectric relaxation time. Actual values have been taken from refs 16b and 20c. No correction was made to account for the electronic charge on the molecule (see: Sumi, H.; Marcus, R. A. *J. Chem. Phys.* **1986**, *84*, 4272).

(53) (a) Simon, J. D. *Acc. Chem. Res.* **1988**, *21*, 128. (b) Maroncelli, M.; MacInnis, J.; Fleming, G. R. *Science* **1988**, *243*, 1674. (c) Barbara, P. F.; Jarzeba, W. *Adv. Photochem.* **1990**, *15*, 1.

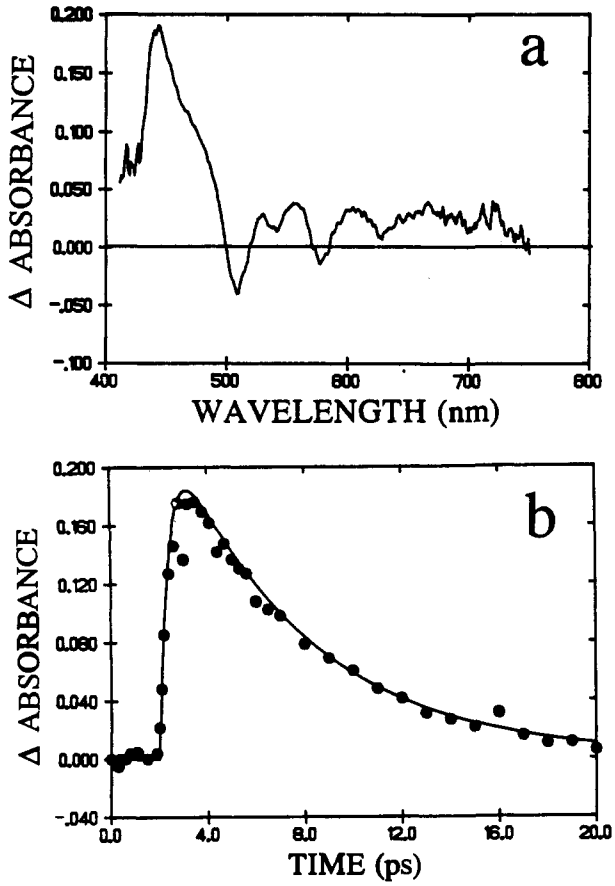

Figure 12. (a) Differential transient absorption spectra recorded 0.5 ps after excitation of **11** with a 0.3-ps laser pulse at 586 nm; the spectra are corrected for spectral chirp. (b) Kinetic trace showing decay of the transient species at 470 nm for the above experiment.

Table 3. Excited Singlet State Lifetimes Measured for the Porphyrin Subunits in the Directly Coupled Binuclear Compounds in Different Solvents and the Corresponding Solvent Reorientation Time

		τ_s (ps)	
solvent	τ_L (ps)	**12**	**11**
CH_3CN	0.5	0.7	5.5
C_3H_7CN	0.7	0.9	4.4
acetone	0.8	1.0	5.0
PC[a]	1.1	1.6	5.7
CH_2Cl_2		0.7	4.6
DMSO[b]	2.1	2.3	6.5
C_6H_5CN	4.8	3.4	7.8
C_2H_5OH	14.0	10.0	18.5

[a] Propylene carbonate. [b] Dimethyl sulfoxide.

changes (ΔG^*) were calculated to be (22 ± 10) cm^{-1} and (375 ± 60) cm^{-1}, respectively, for the zinc porphyrin derivative **12** and the free-base analogue **11** in the rapidly relaxing (i.e., τ_L <3 ps) solvents listed in Table 3. These are modest barriers to electron transfer, being on the order of $0.1k_BT$ and $2k_BT$, respectively, for **12** and **11**, that can be related to the total reorganization energy accompanying electron transfer (λ).[53]

$$\Delta G^* = [\lambda + \Delta G^\circ]^2/4\lambda \qquad (16)$$

This expression allows estimation of λ as *ca.* 4000 cm^{-1} (i.e., 0.5 eV), which is somewhat smaller than the value estimated for the phenyl-bridged binuclear compounds.[54] In terms of the Sumi-Marcus model,[19] electron transfer under these conditions appears to correspond to the situation described by the so-called "narrow" reaction window. That is to say, electron transfer is expected to occur along different solvent coordinates at slightly different rates which depend on the diffusion coefficient (or relaxation time) of the solvent.

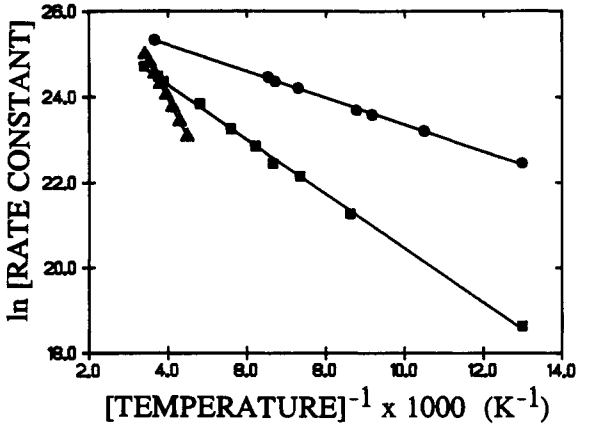

Figure 13. Arrhenius plots for (●) deactivation of the first excited singlet state of the zinc porphyrin subunit in **12**, (■) deactivation for the first excited singlet state of the free-base porphyrin subunit in **11**, and (▲) the solvent reorientation time. All experimental data points refer to ethanol, and the solid lines drawn through the data points are computed nonlinear least-squares fits.

As τ_L increases, however, reaction is expected to move toward the "nondiffusing" limit in which the rate of electron transfer is faster than solvent diffusion.[19] This situation has been observed in several cases and has been examined in detail by Barbara and co-workers[20] for processes occurring within the inverted region. In order to study the effect of increasing τ_L on the rate of electron transfer, the excited singlet state lifetime for each of the directly coupled binuclear compounds was measured in ethanol at low temperatures[55] using time-correlated, single-photon counting techniques. Under such conditions, the decay profiles gave satisfactory fits to single-exponential processes. The results are presented in the form of Arrhenius plots in Figure 13, where it can be seen that both plots are linear over a wide temperature range. This suggests that the activation free energy changes are independent of temperature, despite expected changes in entropy, solvent reorganization energy, solvent relaxation time, or reaction exergonicity as the temperature is lowered. Furthermore, it is apparent that efficient fluorescence quenching persists below the glass transition temperature of the solvent and in a frozen ethanol glass the rates of electron transfer are many orders of magnitude greater than those expected on the basis of eq 15.

Fitting the kinetic data collected in ethanol to eq 15a indicates a common frequency factor of $\alpha = (3.6 \pm 0.4) \times 10^{11}$ s^{-1} and apparent ΔG^* values of (215 ± 15) and (440 ± 30) cm^{-1}, respectively, for **12** and **11**. Figure 13 also provides data relating to the temperature dependence of τ_L, at least over the high-temperature range, where the activation energy (E_L) is (1230 ± 80) cm^{-1}. It appears that at high temperature $k < \tau_L^{-1}$, but, since the various processes possess distinct activation energies, the curves cross such that at lower temperature $k > \tau_L^{-1}$. This suggests, at least from a qualitative viewpoint, that the electron-transfer rate switches progressively from solvent control at high temperature (or in rapidly relaxing solvents) to vibrational dynamic control as the temperature (or relaxation time of the solvent) decreases. Such an effect is predicted by the Sumi-Marcus model[19] where it is considered to arise because electron transfer can proceed along the vibrational coordinates produced in the excitation pulse

(54) The solvent reorganization energy was calculated from dielectric continuum theory to be 6050 and 5160 cm^{-1}, respectively, for the phenyl-linked tripartite and directly coupled binuclear compounds. This calculation usually overestimates the value by as much as 40% (see: Walker, G. C.; Barbara, P. F.; Doorn, S. K.; Dong, Y.; Hupp, J. T. *J. Phys. Chem.* **1991**, *95*, 5712) and, consequently, λ_S values of 3650 and 3100 cm^{-1}, respectively, are considered appropriate for **13** and **12**.

(55) The values for τ_L were taken from ref 16b.

when solvation occurs slowly. We would also expect to observe an enhancement in the rate of electron transfer as τ_L decreases in the high-temperature region, but this effect was not pursued.

Where solvation dynamics are slow with respect to electron transfer (e.g., $\tau_L > 3$ ps) reaction can occur via vibrational modes of the reactant with a rate constant $k(X)$, where X refers to a specific solvent orientation:

$$k(X) = \beta \exp[-\Delta G^*(X)/k_B T] \quad (17)$$

Here, $\Delta G^*(X)$ is the X-dependent activation energy and the frequency factor β is defined by

$$\beta = (2\pi/h)V^2(\pi/\lambda_V k_B T)^{1/2} \quad (18)$$

in the nonadiabatic limit.[19] Using the data displayed in Figure 13 together with estimation[56] of the vibrational reorganization energy $\lambda_V = 3200$ cm^{-1}, we estimate $V \approx 32$ cm^{-1} as averaged over all values of X. The activation energy can be expressed in the form

$$\Delta G^*(X) = [(2\lambda_S)^{1/2}X - (\lambda_V + \lambda_S + \Delta G^\circ)]^2/4\lambda_V \quad (19)$$

The values averaged over all values of X were found to be (410 ± 40) and (550 ± 50) cm^{-1}, respectively, for **12** and **11**.

For the directly coupled binuclear compounds we have studied only the forward reaction, which is expected to lie within the normal region of a rate versus energy gap profile. Charge recombination, however, should be in the inverted region,[57] and, unlike the situation found with the phenyl-linked compounds, is at least as fast as the forward reaction. Barbara and co-workers[20] have shown that the rates of electron-transfer reactions occurring deep in the inverted region can approach τ_L^{-1} in rapidly relaxing solvents and can exceed this limit in slowly relaxing solvents. Even so, the effect of inserting a phenyl ring between the reactants has a dramatic effect on the apparent rates of charge recombination.

(56) This value was derived by assuming that the total reorganization energy calculated for the phenyl-linked tripartite compounds can be divided into vibrational and solvent terms: $\lambda = \lambda_V + \lambda_S$. With $\lambda = 6300$ cm^{-1} and λ_S estimated to be 3100 cm^{-1}, $\lambda_V \approx 3200$ cm^{-1}.

(57) Jortner, J.; Bixon, M. *J. Chem. Phys.* **1988**, *88*, 167; *Chem. Phys.* **1993**, *176*, 467.

Conclusion

This study has shown that metal–bisterpyridyl complexes can quench the excited singlet state of (metallo)porphyrins due to intramolecular electron transfer. With directly coupled reactants, it appears that both forward and reverse electron-transfer steps are extremely fast, and such materials possess little attraction as building blocks. Insertion of a phenyl ring between the reactants has a profound effect on the dynamics of electron transfer, especially charge recombination. The relatively slow rate for charge recombination observed with the ruthenium(II) complex, which arises because of the "inverted effect", suggests to us that this system could be used as a bridge to engineer long-range electron transfer. Thus, attaching a different metalloporphyrin to the open site on the second terpyridyl ligand facilitates formation of a widely spaced, linear bisporphyrin. Selective excitation of one porphyrin chromophore, followed by a two-step electron transfer, might be expected to promote rapid electron transfer over *ca.* 30 Å or so.

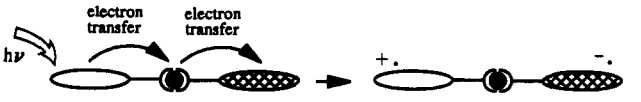

The ruthenium(II)–bisterpyridyl-based system has the additional attraction that light absorbed by the complex is transfered to the triplet excited state of the porphyrin by way of an antenna effect. In properly designed systems, the triplet state will also be capable of effecting long-range, superexchange-mediated electron transfer. Synthesis of such systems is underway and will be reported elsewhere.

Acknowledgment. This work was supported by the NSF (CHE 9102657), NATO (920916), and the CNRS. The CFKR is supported by The University of Texas at Austin. We thank Dr. Keisuke Tominaga for helpful discussions.